21st Australasian Fluid Mechanics Conference
Adelaide, Australia
10-13 December 2018

3D CFD simulation of a turbocharger compressor used as a turbo expander for Organic Rankine cycle

M. Deligant[1], E. Sauret[2], R. Persky[2], S. Khelladi[1] and F. Bakir[1]

[1]Arts et Métiers ParisTech, 151 boulevard de l'Hôpital,75013 Paris, France

[2]School of Chemistry, Physics and Mechanical Engineering I Science and Engineering Faculty (SEF) Queensland University of Technology (QUT), 2 George St, GPO Box 2434, Brisbane 4001 Australia

Abstract

Generating electricity from low grade waste heat resources can contribute to the energy mix required to reduce carbon emissions and dependence on fossil fuels. The conversion of low grade waste heat can be achieved efficiently using Organic Rankine cycles (ORC). Radial-inflow turbine is one suitable technology for the expander in these cycles. The design of such turbines operating with non-ideal gas is challenging and requires advanced modeling techniques to be developed and validated. This paper proposes a novel and cost-effective solution to develop a design approach that combines numerical modeling and experiments. An ORC loop is developed at Dynfluid laboratory for teaching and research purposes. The experimental setup allows experiments of high speed turbines up to 60,000 rpm and 9 kW in a modular way. The first expander to be experimentally and numerically tested will be an adapted compressor from a standard turbocharger. The considered compressor wheel has 6 main blades and 6 splitters blades with an outer diameter of 44 mm and a backswept angle of 45°. The expected performance of the compressor used as a turbo expander are then estimated using 3D CFD real gas simulations and will be ultimately validated against the experimental results. The synergy between numerical modeling and experiments is expected to support the reduction in cost of the manufacturing of turbines prototypes, estimated to represent more than 50% of the total cost of the ORC system.

Introduction

The Organic Rankine cycle allow to convert low grade heat source into electricity. It is well adapted for solar, geothermal, biomass and waste heat recovery. The ORC is usually designed for a specific requirement in terms of temperatures of the resources and available power. This lead to the development of specific expander for each case which is expensive. The spreading of this technology would be accelerated by a cost reduction, especially for small scale system ($< 10kWe$). A way of doing that is to develop standard systems or having systems capable to adapt to various operating conditions. A major problem in developing ORC expanders is the non ideal behavior of the vapor. Although there is a lot of work published on gas turbines, all the models concern ideal gas expansion. The development of the ORC technology focuses on developing design methodology [5, 2, 8], similitude rules [12], 0D 1D loss models ([3, 11, 14]) and CFD models taking into account the non ideal gas behavior of the organic vapor [6, 9], which can all contribute to cost reduction and efficiency gain. The cost reduction in developing new ORC expanders might also be possible by adapting existing parts such are scroll compressors, piston engines, or turbochargers. In 2013, Wong et al. [13] selected a turbocharger's turbine to convert it into a 1 kW ORC turbo-expander. Recently, Deligant et al. [4] designed a solar ORC adapted to a given turbocharger's turbine. The appropriate selection of the ORC operating allow to get similar isentropic efficiency (78%) with organic fluid as with air while optimizing the thermal efficiency of the system. Contrary to the turbine which is usually made of cast iron and inconel alloy, the compressor parts are made with aluminum which is lighter and cheaper. However, the compressor performance with air are unknown in expander mode and therefore cannot be used as reference to convert it into a turbo-expander for organic vapor. In this paper, the compressor of a turbocharger is converted into a turbo-expander for organic vapor, and its performance are predicted using CFD simulations[10].

Original compressor wheel

The considered compressor is extracted from the Garrett GT-15V44 turbocharger. It is typically used for 1.0 to 1.6 liter's engine with an output power ranging from 100 to 150 horse power. The main characteristics of the compressor are presented in table 1. The performance map of this compressor is presented in figure 1. The operating point with best efficiency is considered to be the design point, which characteristics are presented in table 2. The geometry of the compressor is obtained by reverse engineering using Ansys turbo tools Vista CCD. The main dimensions of the compressor are reproduced by adjusting the parameters presented in table 3. The parameters of the obtained geometry are summarized in table 4 and the reproduced geometry compared to the compressor wheel in figure 2.

Trim	72	-
Outer diameter	44.0	mm
A/R	0.33	-
Inner diameter	30.12	mm
Number of blades Z	6 main - 6 splitters	-

Table 1: GT15V44's compressor properties.

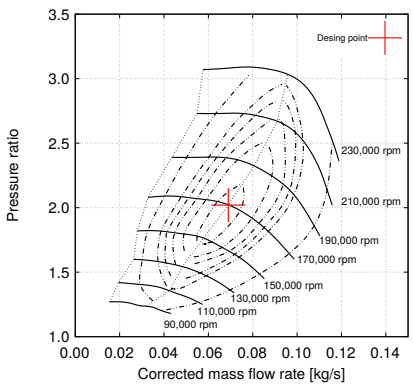

Figure 1: Compressor map - Data extracted from Garrett.

Rotational speed	170,000	rpm
Mass flow rate	0.069	$kg.s^{-1}$
Pressure ratio	2.02	-
Inlet pressure	100,000	Pa
Inlet temperature	293.15	K
Outlet pressure	202,000	Pa
Isentropic efficiency	0.76	-
Power	5.95	kW

Table 2: Data extracted from Garrett and design operating point of the compressor.

Absolute inlet flow angle α_1	70	°
Blade speed ratio	0.6473	-
Shroud exit/inlet ratio	0.849	-

Table 3: Reverse engineering parameters.

Inlet	hub	radius	4.75	mm
		angle	27.89	°
	mid line	radius	11.50	mm
		angle	52.02	°
	shroud	radius	15.55	mm
		angle	60.00	°
	tip		10.8	mm
Outlet	radius		22.00	mm
	angle		45.00	°
	tip		2.66	mm
	Rake angle		30.00	°

Table 4: Geometrical data obtained using ANSYS Vista CCD.

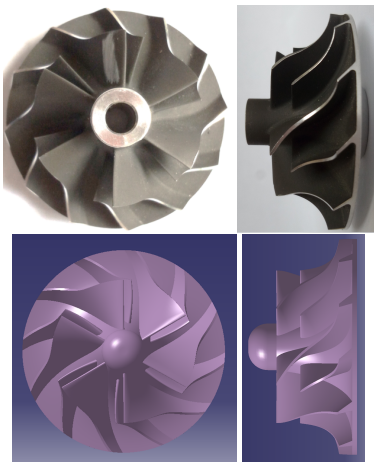

Figure 2: Compressor wheel - Photo and CAD design comparison.

Organic Rankine Cycle

A sub-critical Organic Rankine cycle featuring a heat recuperation is considered (see Fig. 3). The cycle efficiency is expressed by eq (1). It is considered that the heat recuperator allows to transmit 80% of the enthalpy between the end of expansion and the beginning of the condensation.

$$\eta_{cycle} = \frac{(h_2 - h_3) - (h_0 - h_5)}{h_2 - h_1} \quad (1)$$

The working fluid is Solkahterm SES36[1] which is non flammable, has low toxicity and is well adapted for medium temperature ORC [7]. A fixed evaporating temperature of 80°C with a super heating of 20°C are considered. This is an interesting point for both teaching and research and is easily attainable on the experimental loop, with moderate pressure and temperature. The vapor behavior is non ideal with $Z = 0.898$(see fig. 4). The expansion ratio can be varied by adjusting the expander downstream pressure, which is directly linked with the condensation temperature. The rotational speed is set in order to have an inlet Mach number $\mathbf{M} = \frac{U_2}{a_2} = 0.94$. Higher Mach number would generate blockage inside the expander. Lower Mach number would lead to small tangential speed and thus low enthalpy drop (see ref [2]). Given the wheel diameter (44mm) and the inlet sound of speed ($120.35\,m.s^{-1}$), the rotational speed is set to $N = 49,020\,rpm$.

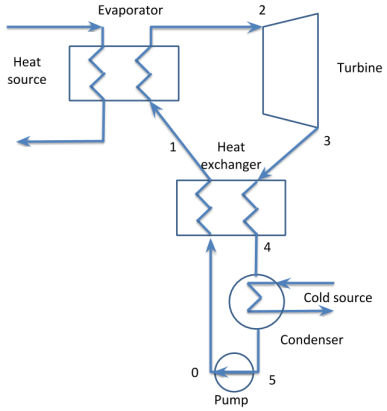

Figure 3: Layout of a generic Organic Rankine cycle with a heat recuperator.

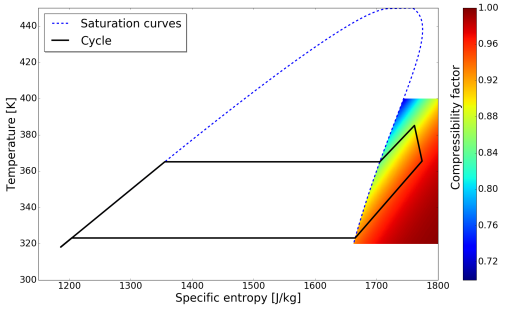

Figure 4: T-s diagram of the cycle with SES36.

CFD simulations

CFD model

Compressible, Frozen rotor simulations were carried out using StarCCM+. The simulations used the standard $k-\varepsilon$ turbulence model [10]. For the simulations with air, the fluid is considered as an ideal gas. For the simulations with SES36, the Peng-Robinson equation of state is considered. The parameters used in the Peng-Robinson equation are presented in Table 5. The boundary conditions are stagnation inlet pressure with a fixed temperature, pressure outlet and adiabatic walls. Note that the surface considered as inlet and outlet are modified when chang-

ing from compressor mode to expander simulations. The direction of the rotation is also reversed.

Mesh

The mesh used the polyhedral mesher with a base size of 2 mm and a prism layer of 3 cells.

The total number of nodes is 515,272. The average non-dimensional grid spacing at the walls is $y_{+w} = 35$ for simulation with air and $y_{+w} = 160$ for simulations with SES36. A picture of the mesh is presented in figure 5.

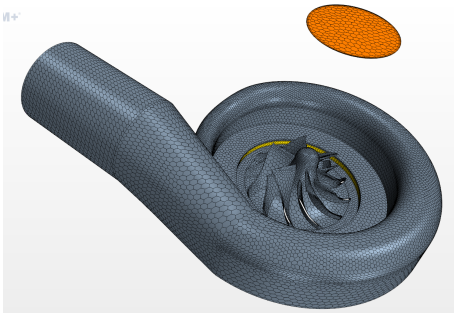

Figure 5: Overview of the mesh.

Property	Units	SES36
Molecular Weight	$g.mol^{-1}$	0.18485
Critical Temperature	K	450.70
Critical Pressure	bar	28.49
Acentric Factor	-	0.352

Table 5: Parameters of the Peng Robinson equation.

Results

The convergence of the computation is ensured by monitoring residuals decrease and asymptotic behavior of integral values such as torque, efficiency and outlet mass flow rate. In a first step, the reverse engineering of the compressor is validated by comparing the performance from the experimental compressor map and the CFD results (fig. 6). It can be noticed that experimental data and the CFD results are in good agreement for 170,000 rpm especially around the nominal point. At low flow rate the obtained pressure ratio is higher than expected. It is a bit lower for high mass flow rates. The difference might come from the error in estimating the backswept angle. The actual blade angle of the compressor is probably slightly lower than the 45°used, which would reduce the slope of the performance curves. The CFD results show a higher pressure ratio for 190,000 rpm. The difference might come from the fact that the tip clearance has been neglected in the CFD simulations. This hypothesis has more importance at high pressure ratio and high velocity speed.

The simulations with organic vapor in expander mode present an optimal operating point with a pressure ratio of 1.74, an isentropic efficiency of 61.2% and a condensation temperature of 59.86°C, as shown in figure 7. For these parameters the cycle efficiency is 3.33% and 2.91% without the heat recuperator. This efficiency may seem low, but in that case the hot source is around 100°C, and the temperature difference is only about 45°C. This cycle with its turbine might be well suited for solar combined heat and power applications. As the inlet conditions are fixed, the outlet pressure decrease with the increase of the

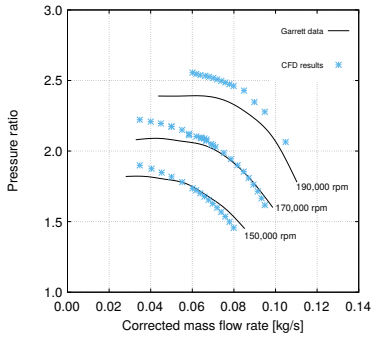

Figure 6: Compressor map - CFD results comparison with experimental data from Garrett.

pressure ratio. Thus, the corresponding condensation temperature of SES36 is reduced.

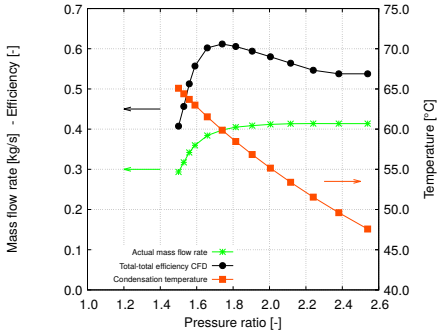

Figure 7: ORC turbine performance curve at $N = 49,020\,rpm$ with fixed inlet conditions $P_1 = 3.84\,bar$ and $T_1 = 373.15$.

The Mach number contours at mid height of the inlet of the wheel are presented in figure 8. Although the flow is transonic at the blade tip, there is no blockage of the flow. The sound of speed increases with the expansion of the vapor. With the reduction of the pressure ratio, the condition at the wheel inlet are closer to the condition at the nozzle inlet, the sound of speed is then lower and thus the Mach number higher.

The relative velocity vectors are presented in figure 9. It can be noticed that the velocity vectors are well aligned with the blade for the nominal pressure ratio b). The flow is less adapted for higher pressure ratio c) with the presence of vortex and for lower pressure ratio a) with the presence of a jet which generates incidence losses.

Conclusions

In this paper, the compressor of a standard turbocharger has been studied for its potential use as a turbo expander for an ORC. For the selected fluid and a given set on inlet conditions, the outlet pressure has been varied in order to obtain the performance curve. The considered expander has a peak efficiency at 61.2% which allows the design of a recuperated ORC with a thermal efficiency of 3.33%, and demonstrates the interest of using a standard compressor to establish a workable and cheap ORC. The future work will focus on adapting this standard compressor to physically test it on the ORC experimental loop available at Arts et Métiers ParisTech. The design of the mechanical connection with the high speed generator will be required and a solution for the sealing problem will be needed. To reproduce the CFD results, the tests will have to be carried out varying the condensation temperature by either adjusting the subcool-

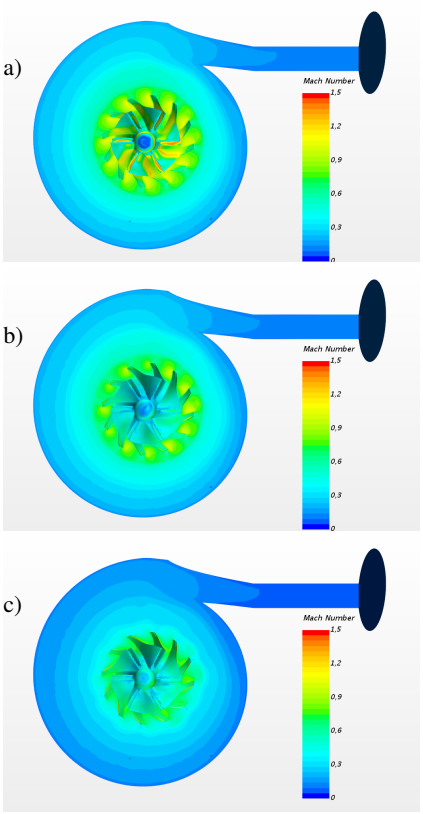

Figure 8: Mach Number at three different pressure ratios a) 1.47, b) 1.74 and c) 2.38.

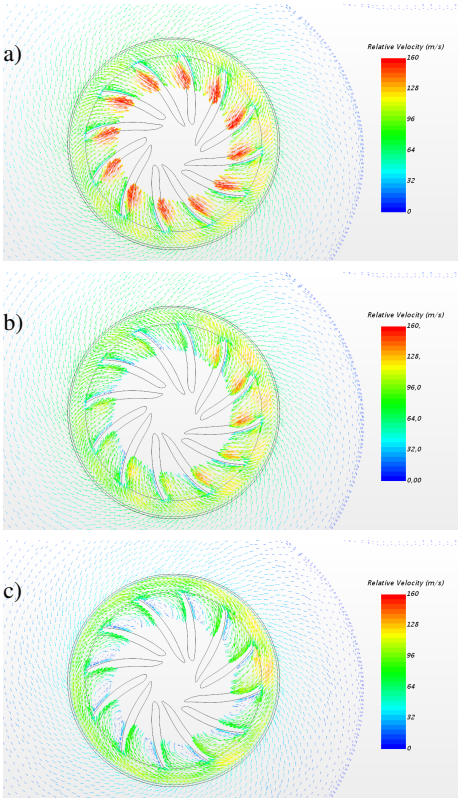

Figure 9: Velocity field for three different pressure ratio a) 1.47, b) 1.74 and c) 2.38.

ing and/or the quantity of fluid in the loop.

References

[1] SOLKATHERM SES 36 Safety datasheet, 2015.

[2] Costall, A., Gonzalez Hernandez, A., Newton, P. and Martinez-Botas, R., Design methodology for radial turbo expanders in mobile organic Rankine cycle applications, *Applied Energy*, 1–15.

[3] Da Lio, L., Manente, G. and Lazzaretto, A., A mean-line model to predict the design efficiency of radial inflow turbines in organic Rankine cycle (ORC) systems, *Applied Energy*, **205**, 2017, 187–209.

[4] Deligant, M., Danel, Q. and Bakir, F., Performance assessment of a standard radial turbine as turbo expander for an adapted solar concentration ORC, in *Energy Procedia*, 2017, volume 129.

[5] Fiaschi, D., Manfrida, G. and Maraschiello, F., Design and performance prediction of radial ORC turboexpanders, *Applied Energy*, **138**, 2015, 517–532.

[6] Harinck, J., Guardone, A. and Colonna, P., The influence of molecular complexity on expanding flows of ideal and dense gases, *Physics of Fluids*, **21**.

[7] Kaya, A., Lazova, M. and Paepe, M. D., Design and Rating of an Evaporator for Waste Heat Recovery Organic Rankine Cycle Using SES36, *Proceedings of the 3rd International Seminar on ORC Power Systems*, 1–10.

[8] Kim, I. S., Kim, T. S. and Lee, J. J., Off-design performance analysis of organic Rankine cycle using real operation data from a heat source plant, *Energy Conversion and Management*, **133**, 2017, 284–291.

[9] Pini, M., De Servi, C., Burigana, M., Bahamonde, S., Rubino, A., Vitale, S. and Colonna, P., Fluid-dynamic design and characterization of a mini-ORC turbine for laboratory experiments, *Energy Procedia*, **129**, 2017, 1141–1148.

[10] Sauret, E. and Gu, Y., 3D CFD SIMULATIONS OF A CANDIDATE R143A RADIAL-INFLOWTURBINE FOR GEOTHERMAL POWER APPLICATIONS, *Proceedings of the ASME 2014 Power Conference*.

[11] Sauret, E. and Rowlands, A. S., Candidate radial-inflow turbines and high-density working fluids for geothermal power systems, *Energy*, **36**, 2011, 4460–4467.

[12] White, M. and Sayma, A. I., The application of similitude theory for the performance prediction of radial turbines within small-scale low-temperature organic Rankine cycles, *Journal of Engineering for Gas Turbines and Power*, **137**, 2015, 10.

[13] Wong, C. S., Meyer, D. and Krumdieck, S., Selection and Conversion of Turbocharger As Turbo-Expander for Organic Rankine Cycle (Orc), *35th New Zealand Geothermal Workshop*, 1–8.

[14] Zheng, Y., Hu, D., Cao, Y. and Dai, Y., Preliminary design and off-design performance analysis of an Organic Rankine Cycle radial-inflow turbine based on mathematic method and CFD method, *Applied Thermal Engineering*, **112**, 2017, 25–37.